Determining the size of lightning-induced electron precipitation patches

Mark A. Clilverd,[1] David Nunn,[2] Sean J. Lev-Tov,[3] Umran S. Inan,[3]
Richard L. Dowden,[4] Craig J. Rodger,[4] and Andy J. Smith[5]

[1]   We analyze Trimpi signatures during 23 and 24 April 1994 at four sites on or near the Antarctic Peninsula (Palmer, Faraday, Rothera, and Halley) on subionospheric VLF signals received from four U.S. naval transmitters (NAA, NSS, NLK, and NPM). Electron precipitation patches are found to be large, i.e., $\sim$1500 km $\times$ 600 km, with the longer axis oriented east-west. Calculations using a three-dimensional Born scattering model, where patch densities are 1.5 electrons cm^{-3} above ambient at the center at $\sim$84 km altitude, provides results that are consistent with this picture. A high proportion (38%) of the Trimpi events were associated with strong lightning flashes in eastern United States. When lightning discharges had currents >65 kA (positive or negative), there was a >80% chance of seeing an associated Trimpi event. The chance of seeing any Trimpi events fell to near zero for discharges of <45 kA. The largest Trimpi perturbations occur when the center of the precipitation patch is 700–800 km from the receivers. This result is consistent with the modeling calculations for large patches. The equatorward edge of the precipitation patch was estimated to be at $\sim$60°S, close to the magnetic conjugate of the lightning. The close association of the equatorward edge of the precipitation patch with the conjugate location of the causative lightning is consistent with a quasi-ducted whistler-induced precipitation mechanism. Nonducted whistler-induced precipitation mechanisms would predict a 5°–10° latitudinal gap between the lightning and the equatorward edge of the patch. However, the lack of observed whistlers at the time of the Trimpi events is consistent with the nonducted whistler mechanism and is not consistent with the quasi-ducted mechanism, although the distances from duct exit point to receiver may have been too large ($\sim$700–1000 km) for the signals to be detectable. Using the significantly larger patch dimensions determined in this study, it is estimated that lightning may well be 10–100 times more effective at depleting the radiation belts than hiss.   INDEX TERMS: 2455 Ionosphere: Particle precipitation; 2716 Magnetospheric Physics: Energetic particles, precipitating; 3324 Meteorology and Atmospheric Dynamics: Lightning; 6964 Radio Science: Radio wave propagation; KEYWORDS: lightning, precipitation, Antarctica, Trimpi, whistler

1.   Introduction

[2]   The Trimpi effect is a well-known phenomenon in radio science and consists of transient perturbations in amplitude and phase of a received narrowband subionospheric VLF/LF signal. Such signal perturbations are known to be due to localized D region inhomogeneities or lightning-induced electron precipitation (LEP) produced ionization enhancements (LIEs), comprising perturbations in electron density and possibly collision frequency [Helli-well et al., 1973]. The energetic electron precipitation arises from lightning whistlers interacting with cyclotron resonant radiation belt electrons in the equatorial zone.

[3]   Determining the typical size of LEP patches would allow the calculation of electron precipitation fluxes following wave-particle interactions [Nunn and Strangeways, 2000]; input into modeling the dimensions of plasmaspheric ducts [Strangeways, 1999]; and investigation of the possibility of oblique (nonducted) whistler-induced precipitation [Lauben et al., 1999; Johnson et al., 1999].

[4]   Previous estimates have suggested patch sizes of the order of 50 km $\times$ 200 km, with the major axis lying parallel to lines of constant L shell. Since early estimates were made by Crombie [1964] and then Tolstoy and Rosenberg [1986], increasingly sophisticated computer modeling and experimental setups have been used to refine the picture. Dowden and Adams [1989] found strong diffraction regions caused by patches less than 50 km wide in latitude, although considerably more in longitude. Similarly, Smith et al. [1993] and Smith [1996] used Trimpi signatures observed

[1]Physical Sciences Division, British Antarctic Survey, Cambridge, England, UK.
[2]University of Southampton, Southampton, England, UK.
[3]STAR Laboratory, Stanford University, Stanford, California, USA.
[4]Low Frequency Electromagnetic Research Ltd., Dunedin, New Zealand.
[5]Physical Sciences Division, British Antarctic Survey, Cambridge, England, UK.

in the Antarctic Peninsula region to infer perturbed regions of the ionosphere with dimensions of 50 km latitudinally and 200–300 km longitudinally. *Poulsen et al.* [1993] suggested the need for ionospheric disturbances of radius 50–200 km in order to scatter a measureable signal. Using a network of receivers, *Dowden and Adams* [1993] found that most LIEs had latitudinal dimensions of 100–250 km, with longitudinal dimensions being much larger. However, some of the events observed in that study were consistent with smooth lateral spread, but the remainder required fine structure to explain the observed diffraction patterns. The interpretation of the results of these early studies were made more complex by the realisation that non-LEP Trimpi (some of which appear to be associated with red sprites) were contaminating the studies [*Rodger*, 1999; *Nunn and Strangeways*, 2000].

[5] More recently, *Dowden et al.* [2001] used the decay timescale information from Trimpi signatures to determine the dimensions of LEP and non-LEP patches. LEP patches were found to be thin (20 km vertically) and significantly larger than in earlier work (300 km×1000 km). In contrast, non-LEP patches have significant vertical extent but are only 25–50 km in horizontal extent. Further indications of large LEP patch dimensions came from *Lauben et al.* [1999] and *Johnson et al.* [1999] where the inferred spatial extent of ionospheric disturbance from precipitation caused by obliquely (nonducted) propagating whistlers was ~1000 km. Large patch dimensions have also been suggested by *Strangeways* [1999] through a quasi-trapped whistler propagation theory in which ducted energy spreads at the magnetic equator. This produces a significantly larger precipitation footprint than the actual dimensions of the plasmaspheric duct.

[6] In this paper we analyze Trimpi signatures received during 23 and 24 April 1994 at rour sites on the Antarctic Peninsula (Palmer, Faraday, Rothera, and Halley). Subionospheric VLF signals were received from four U.S. naval transmitters (NAA, NSS, NLK, and NPM). We analyze a small representative subset of Trimpi events in detail but also consider data collected from March–October in 1994 and 1995 in order to relate the small data set to typical Trimpi characteristics. The Trimpi analyzed in this study were generated following the occurrence of lightning in North America. Local sources of lightning that might produce non-LEP signatures in the data sets are extremely rare in the Antarctic [*Ingmann et al.*, 1985]. Three-dimensional (3-D) modeling is used to calculate the patch dimensions and hence investigate the likelihood of ducted or non-ducted VLF waves being responsible for the production of electron precipitation patches.

2. Experimental Setup

[7] Subionospheric signals from VLF transmitters were recorded on OMSK receivers [*Dowden et al.*, 1994] at Faraday (65.3°S, 64.3°W), Rothera (67.5°S, 68.1°W), and Halley (75.5°S, 26.5°W), Antarctica [*Clilverd et al.*, 1999]. The phase and amplitude of the signals were logged with a time resolution of 0.4 s. The phase and amplitude receiver used at Palmer (64.8°S, 64.1°W) is described by *Lev-Tov et al.* [1995] and was run with a time resolution of 0.1 s. The transmitters studied were NAA (24.0 kHz, Cutler, Maine),

NSS (21.4 kHz, Annapolis, Maryland), NLK (24.8 kHz, Seattle, Washington), and NPM (23.4 kHz, Oahu, Hawaii). Palmer monitored NAA, NSS, NLK, and NPM. Faraday monitored NAA and NPM. Rothera monitored NAA, NSS, and NLK. Halley monitored NAA and NSS. Thus 10 great circle paths (GCPs) criss-cross the region of the Antarctic Peninsula where precipitation is expected to occur initiated by continental lightning in the United States [*Burgess and Inan*, 1993; *Lev-Tov et al.*, 1996; *Clilverd et al.*, 1999]. The locations of the receivers and the GCPs to the transmitters are shown in Figure 1. The $L = 2.0$ and $L = 2.5$ contours are also shown (dashed lines). An ellipse is plotted to indicate the possible size and shape of the region into which electron precipitation is likely to be occurring in the Trimpi events studied in this paper.

[8] The Trimpi observed were analyzed using a simple algorithm to determine the size of the changes in amplitude and phase of the transmitter signals. The significance of the Trimpi events were estimated based on the maximum change of amplitude compared with the noise levels occurring at the time of the event. A best fit regression line through the data points is determined for before and after the event time, using 11 samples before and after (either 0.4 or 1.25 s per sample). Separate regression lines, deviations, and differences at $t = 0$ intercept are calculated for the phase and amplitude, which are then combined (linearly) to detemine the significance parameter. Typical significance values of 1000–2000 occur for well defined Trimpi events. Examples of a range of values are shown in Figure 2, where the long-dashed lines represent the best fit regression line, and the vertical short-dashed line represents the $t = 0$ intercept. The significance of the Trimpi (effectively the signal/noise) increases as the Trimpi effect becomes larger and more well defined. Clearly, the bottom panels of Figure 2 show a Trimpi that has the largest amplitude and phase changes, and the least noise. Thus the significance value is the highest. Significance values of <500 are not considered as indicating the presence of a Trimpi. The significance of the Trimpi observed will be discussed in section 3.

[9] In this study we are concerned only with Trimpi caused by LEP. As such, any non-LEP Trimpi occurring at the transmitter end of the GCP could contaminate the data sets. Non-LEP Trimpi are produced by ionospheric disturbances directly associated with lightning and can be expected for transmitters in the mainland United States and Hawaii. Lightning is very rare in Antarctic Peninsula region, and thus we do not expect local non-LEP Trimpi to appear in the study. By only selecting Trimpi events that were simultaneously observed on the majority of the GCPs mentioned above we can be confident that the ionospheric disturbance is located in the Antarctic Peninsula region and hence can only be caused by LEP.

3. Observational Results

[10] The phase and amplitude changes associated with an isolated Trimpi event observed at 0547 UT on 23 April 1994 are shown in Figure 2. The plot shows NAA at Faraday, NSS at Rothera, NLK at Rothera, NPM at Palmer, and NPM at Faraday. A clear Trimpi signature is observed at 0547:05 UT on all of the paths, both in phase and amplitude. The onset of the Trimpi event is simultaneous
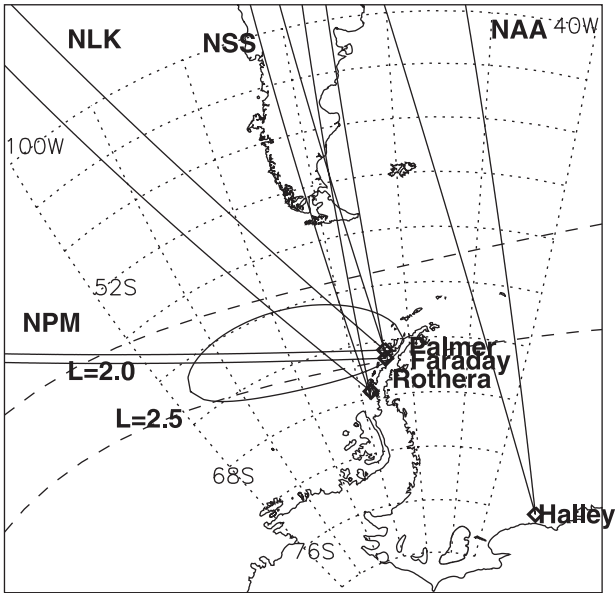
Figure 1. A map of the region around the Antarctic Peninsula. The location of the Palmer, Faraday, Rothera, and Halley receivers are indicated. The Great Circle Paths to the transmitters studied are plotted, along with the $L = 2.0$ and $L = 2.5$ contours at 100 km altitude. An ellipse marks the possible size and location of an electron precipitation patch producing a Trimpi event observed at the receivers.

on all paths to within ±1 s. A second smaller Trimpi event can be seen occurring at 0547:24 UT.

[11] The interpretation of simultaneous Trimpi event occurrence on all paths is either one of a large patch of precipitation covering the whole region, or of several smaller patches that individually interact with separate paths. Potentially, small patches of ionization could be caused by multicomponent whistlers. However, small patches of ionization would be expected to produce Trimpi events with a variety of phase and amplitude relationships. Small patches distributed over a range of distances from GCPs would give a wide ranging distribution of phase versus amplitude in a scatter plot [*Dowden and Adams*, 1989]. In this study we analyzed ~1000 Trimpi events during 1994 and 1995. There were never less than 5 GCPs recorded, always covering the whole of our study region. The vast majority of the events (>95%) exhibited consistent phase and amplitude relationships on any path that showed an effect, i.e., positive phase, negative amplitude for NPM at Faraday [*Clilverd et al.*, 1999]. These relationships are given in Table 1, which shows the typical phase and amplitude relationships observed for the nine GCPs logged during this study. In general, the paths to the north of the receivers showed positive amplitude and positive phase events, while paths to the northwest and west showed negative amplitude and positive phase. This finding provides convincing evidence for a single large patch.

[12] For the purposes of comparison with several different paths it is more efficacious to plot scatter phase, which is the phase between the scattered signal and the GCP direct signal, and scatter strength, which is the ratio, in decibels, between the strength of the scattered field and the GC path

direct signal. The relationships between amplitude and phase Trimpis and scatter strength and scatter phase are well known and readily derived [*Dowden and Adams*, 1988; *Wolf and Inan*, 1990]. The scatter strength and phase of a representative subset of the events taken from 23 and 24 April 1994 are given in Table 2. Group a is representative of the Trimpi events that occurred on 23 April and group b representative of 24 April. All the events shown had amplitude and phase characteristics consistent with the relationships shown in Table 1.

3.1. Location of Causative Lightning

[13] If we can determine the typical location of the causative lightning flash, this should provide some information on the likely location of the precipitation patch. If the precipitation is caused by nonducted VLF waves, then we should expect the precipitation to occur on the same longitude as the flash, but probably poleward [*Johnson et al.*, 1999]. If the precipitation is caused by ducted VLF waves then the patch could be offset latitudinally either side of the causative lightning location. However, on average, the location of the duct would be close to the longitude of
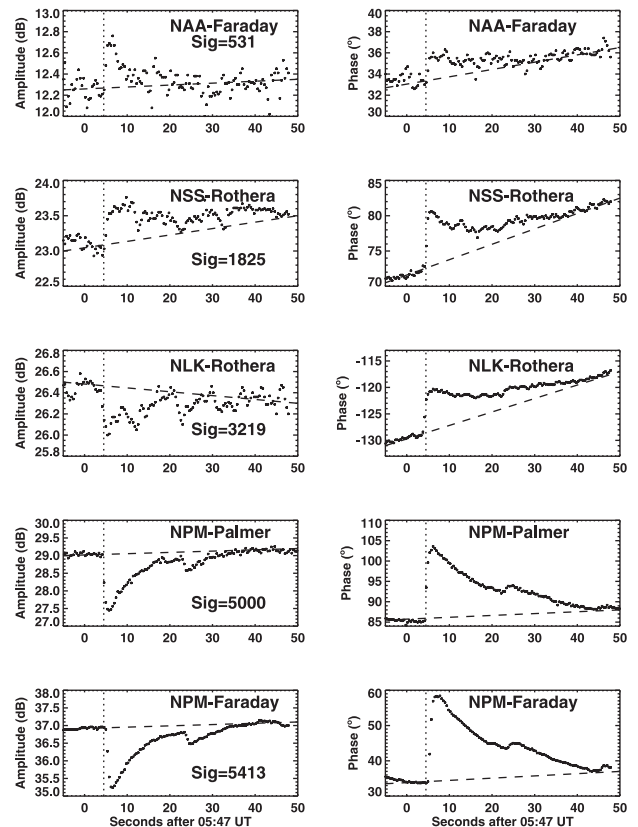

Figure 2. An example of a Trimpi event observed on several paths during 0547 UT on 23 April 1994. The time resolution is 0.4 s. The onset time of the Trimpi event is indicated by a vertical dashed line. Significant changes in amplitude and phase occur at the beginning of the event and typically last for 30–40 s. The unperturbed behavior of the signals is indicated by the long dashed lines. The significance of the perturbation is also shown, higher values representing better signal/noise − see text for more details.

Table 1. Sign Relationship of the Trimpi Events Received on the Antarctic Peninsula

GCP	Bearing, °W of N at Rx	Amplitude, dB	Phase, deg
NAA-Palmer	2	+ve	+ve
NAA-Faraday	2	+ve	+ve
NAA-Rothera	1	+ve	+ve
NSS-Palmer	10	+ve	−ve
NSS-Rothera	9	+ve	+ve
NLK-Palmer	41	−ve	+ve
NLK-Rothera	42	−ve	+ve
NPM-Palmer	84	−ve	+ve
NPM-Faraday	84	−ve	+ve

the lightning, although probably slightly poleward to facilitate efficient coupling [*Strangeways*, 1981].

[14] To locate the lightning discharges likely to result in Trimpi events observable from the Antarctic Peninsula, we analyzed lightning data from the coastal region of eastern United States. The U.S. National Lightning Detection Network (NLDN) has operated since 1989. A network of ≈106 receiving stations is connected to a central processor that records the time, polarity, signal strength (proportional to peak current), and number of strokes of each cloud-to-ground lightning flash detected over the continental United States [*Cummins et al.*, 1998]. NLDN is designed to have data from an average of six to eight sensors contributing to the determination of the location of a stroke. The detection efficiency during the period of interest in this paper (April 1994) is estimated to have been 70–80% for return stroke peak currents of 5 kA or more, with a typical location accuracy of 2–4 km over the United States, falling to 8–16 km at 200–400 km offshore.

[15] During 0500–1100 UT of 23 and 24 April 1994 we looked for the occurrence of large lightning flashes and checked to see if a Trimpi event was observed a second or two later on the Antarctic peninsula. For flashes with currents >100 kA, there were 44 agreements versus 2 occasions where such high-current lightning occurred, but no Trimpi were seen during good, low noise, receiving conditions. This finding is consistent with the findings of earlier work, where *Inan et al.* [1988] found that 25 large lightning discharges could be associated with Trimpi events on all but 1 occasion. *Burgess and Inan* [1990] also found a close association between Trimpi events on NPM-Palmer and lightning occurring in eastern United States. The two lightning flashes without corresponding Trimpi signatures in this study had
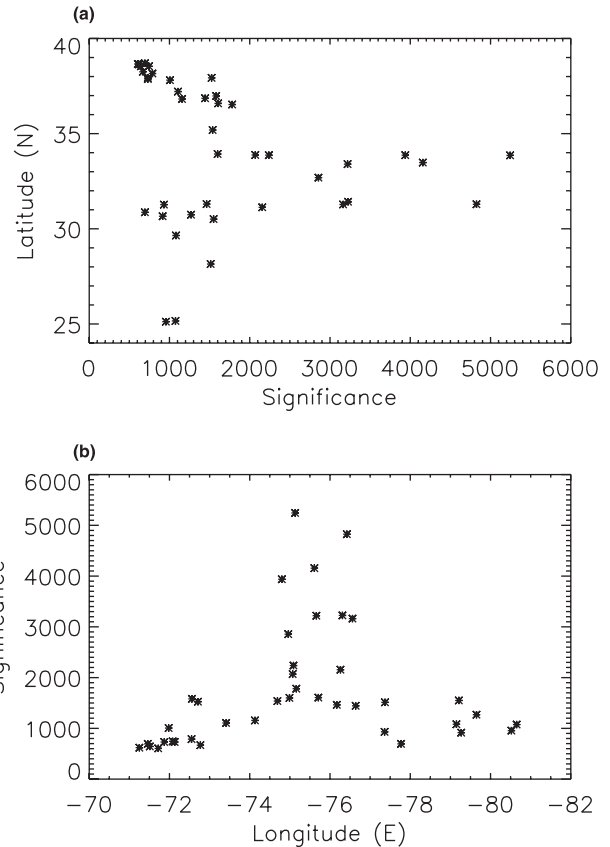

Figure 3. The variation of Trimpi Significance on NPM-Faraday compared with the latitude and longitude of the causative discharge.

latitudes of between 26° and 8°N, significantly south of the conjugate region to Faraday (38°N) and may mark the farthest end of the latitude range for detectability from the Antarctic sites of the resultant precipitation events. Figure 3 shows the significance values of Trimpi events observed on NPM-Faraday against latitude (Figure 3a) and longitude (Figure 3b) of the lightning discharge. There are increasing significance trends as the flashes occur toward 34°N, 76°W, with relatively small significance values when flashes occur elsewhere. The conjugate location to this region is 60°S, 80°W, which is to the west of the Antarctic Peninsula. The center of a precipitation patch resulting from the lightning

Table 2. Scatter Amplitude (Sc-A) and Phase (Sc-P) of a Representative Subset of the Trimpi Events Observed on 23 and 24 April 1994[a]

Date	Time, UT	NAA-Faraday Sc-A Sc-P, db/deg	NSS-Rothera Sc-A Sc-P, db/deg	NLK-Palmer Sc-A Sc-P, db/deg	NLK-Rothera Sc-A Sc-P, db/deg	NPM-Faraday Sc-A Sc-P, db/deg	NSS-Halley Sc-A Sc-P, db/deg
				Group A			
23 Apr 94	0547:06	−23.0 +35	−15.9 +71	−20.8 +103	−17.5 +111	−7.3 +128	. . . . . .
23 Apr 94	0549:02	−30.6 +39	−20.0 +59	−25.2 +105	−22.9 +101	−12.9 +124	. . . . . .
23 Apr 94	0550:17	−30.1 +64	−20.3 +84	−25.1 +106	−22.4 +109	−12.5 +125	. . . . . .
23 Apr 94	0608:04	. . . . . .	−20.0 +64	. . . . . .	−18.8 +128	−5.8 +135	. . . . . .
				Group B			
24 Apr 94	0816:29	−9.2 +56	−19.6 . . .	−20.2 +126	−16.1 +151	−14.5 +133	−20.3 +314
24 Apr 94	0853:44	−17.1 +48	. . . . . .	−25.2 +127	−23.3 +153	−17.5 +118	−21.6 +317
24 Apr 94	0855:57	−14.7 +59	. . . . . .	−21.6 +129	−21.0 +153	−15.9 +119	−18.6 +294
24 Apr 94	0857:09	−18.5 +56	. . . . . .	−22.4 +110	−25.8 +165	−19.0 +119	−22.0 +316

[a] The dashed lines mean that no clear measurement could be made, either due to high noise levels or too small an effect.
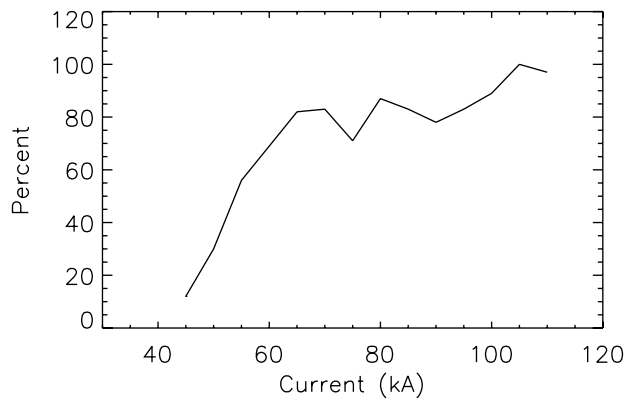
Figure 4. The percentage of Trimpi events associated with lightning discarges in eastern United States versus the current of the discharge (positive or negative) in 5-kA bins.

[Lauben et al., 1999; Strangeways, 1999] would be expected to be poleward of this location. At 65°S the longitude of 80°W is ~700 km from the Faraday receiving site.

[16] During 0500–1100 UT on 23 April 1994, 334 Trimpi events were observed on NPM-Faraday. Only 42 Trimpi events were immediately preceded by flashes where the discharge current was >100 kA (positive or negative). Of the other 292 events, 84 are associated with recorded discharges in the eastern United States. The causative discharges for the remaining Trimpi events probably occur out to sea, which is too far eastward to be seen by NLDN. This is confirmed by the detection of simultaneous Trimpi events occurring on the NSS-Halley GCP, which is more easterly than the other paths discussed here. Figure 4 shows the percentage of discharges that have been associated with a Trimpi event versus the current of the discharge. The bins are 5 kA wide. The percentage association falls rapidly toward zero at ~50 kA (positive or negative). This may represent the lower limit of the wave amplitude for whistlers interacting with cyclotron resonant radiation belt electrons. For discharges above 65 kA there is a good chance of seeing a coincident Trimpi event (>80%).

[17] The Trimpi events that occur during 0800–0900 UT on 24 April 1994 appear to be caused by lightning flashes from eastward of the region of maximum significance, possibly 65°–70°W. Evidence for this is that we observe Trimpi events on all the usual paths plus NAA-Halley and NSS-Halley (see Table 2). The Halley paths cross the $L = 2.5$ contour at ~50°W. In addition, no coincident large lightning flashes were detected close to the eastern sea board, the inference being that the flashes were farther out to sea and not detected. The significance on NPM-Faraday for these Trimpi is only 3000, compared with the maximum of 5500 shown in Figure 3. We assume this is because the patch of precipitation has significant area to the east of Faraday compared with the other Trimpi events, and thus produces less effective Trimpi events on the westerly NPM-Faraday path. At 65°S the longitude of 50°W is ~650 km from the Faraday receiving site.

3.2. Estimates of Patch Size

[18] The simplifying assumpton made here is that the scatter amplitude of Trimpi events is proportional to the length of the GCP through the patch itself. This is likely to be true for large smoothly varying patches, but not true for small denser patches. However, we believe that the evidence presented in Table 1 is highly suggestive of large patches, and therefore we continue with that assumption in place. During 23 and 24 April 1994 ~400 Trimpi events were analyzed in detail. Table 2 gives details of a representative subset of these events which occur to the west of Faraday on April 23, group a, or close to overhead on April 24, group b.

[19] In group a the east-west path, NPM-Faraday, typically observes Trimpi events of ~−10 dB. This is much larger than the north-south path, NSS-Rothera, which typically observes −18 dB events. Thus the horizontal dimensions of the region of ionization on the path must be larger east-west than north-south, with the ratio being a factor of ~2.5. The most easterly path, NAA-Faraday, has Trimpi events that are typically −26 dB and probably represents the eastern edge of the patch. No events in this group were observed on the far eastern path, NSS-Halley. Lightning flashes can be associated with some of these events and they are located around 33–34°N, 75–76°W. If the middle of the patch is close to the conjugate longitude of the lightning flash determined above we would estimate the major axis of the patch to be of the order of 1500 km (twice the distance of patch center to Faraday) and the minor axis of the order of 600 km. The Trimpi events on 23 April 1994 that occurred before the start of daylight conditions (≈11 UT) all gave similar results regarding patch dimensions.

[20] However, the Trimpi events in group b on 24 April 1994 could not be associated with an NLDN-observed lightning flash on the east coast of USA. This is probably because the lightning conjugate is much nearer to the longitude of Faraday than the example described immediately above, and hence beyond the NLDN detection area. This is consistent with the fact that these are the Trimpi that were observed simultaneously on the Halley paths. The perturbation observed on the NLK-Rothera path is this time smaller than that on NAA-Faraday, suggesting that the patch effects a smaller amount of path to the west of the peninsula than paths directly north of Faraday, again consistent with the center of the patch being near Faraday. In fact, the westerly path, NPM-Faraday, has basically the same scatter values as the northerly path, NAA-Faraday, suggesting that the patch is as wide in latitude as it is in longitude to the west of Faraday. To the west the NLK-Rothera path crosses the $L = 2.5$ contour ~500 km from Faraday. To the east the NSS-Halley path is 650 km distant. This suggests that the major axis is at least ~1200 km and that the ratio for the major:minor axis is ~1200:500 or a factor of 2.4.

[21] In the above representative examples we have described the process by which precipitation patch sizes were estimated. Using Trimpi events on 23 and 24 April 1994, we estimate the precipitation patch sizes to be ~1500 km by ~600 km. Typically, they are centered to the west of the Antarctic Peninsula by ~700 km, although they can be much closer at times. The next section describes the modelling processes used to investigate the relationships shown in Tables 1 and 2 using a 3-D Born Trimpi scattering model, and a patch of similar size and shape to that estimated above.

4. Modeling

4.1. LIE Scattering Model

[22] The direct transmission paths for which numerical modelling will be made are NPM, NSS, NAA, and NLK to Faraday, Antarctica. Separate computations will not be made for a receiver at Palmer, which is very close to Faraday. Rothera station is some 300 km to the SW of Faraday, and again separate computations need not be made, provided that the location of the patch relative to the GCP is adjusted appropriately. GCP data required for these computations are as follows: (1) NPM–Faraday; f = 23.4 kHz; range = 12.3 Mm; GCP bearing to Faraday 96° with respect to magnetic North. (2) NAA–Faraday; f = 24.0 kHz; range is 12.2 Mm; GCP bearing 178°. (3) NSS–Faraday; f = 21.4 kHz; range is 11.6 Mm; GCP bearing 170°. (4) NLK–Faraday; f = 24.8 kHz; range is 13.6 Mm; GCP bearing 138°.

[23] The transmitters are modeled as vertical electric dipoles at zero altitude. The receiver at Faraday is assumed to be a vertical electric dipole, though in experimental practice the horizontal magnetic fields are measured. The computer code for the numerical modeling of the VLF Trimpi effect is fully three dimensional with an anisotropic ionosphere and curved earth, and is based upon a linear weak scattering or Born formalism. The code is very general and has been used to successfully model VLF scattering not only from "classical" LIEs as here, but also from a time decaying red sprite plasma column [*Nunn and Rodger*, 1999] and from assemblies of spritelet plasma columns [*Rodger and Nunn*, 1999]. Apart from the LIE itself the background ionosphere is assumed to be homogeneous. This presents some difficulties for the present computations since the GC path and transmitter–LIE paths are always very long (~12 Mm). The ambient ionospheric profile and, of course, ambient magnetic field vector will vary considerably over this distance making the incident complex modal composition vector at the LIE hard to accurately predict. The ground properties also are assumed to be homogeneous and to have the properties of seawater with a conductivity of 0.20 S m^{-1} and a dielectric constant of 81. The region of direct interest is entirely over the sea, but in the case of the long paths from NAA and NSS, there are substantial overland segments. Furthermore, these paths encounter ionospheric inhomogeneities related to the South Atlantic Anomaly. The unperturbed ionospheric electron density and collision frequency profiles are given by a standard nighttime ionospheric model. The collision frequency (ν) profile is given as a function of vertical coordinate z, by

$$\nu(z) = 1/\tau(z) = 1.86 \times 10^{11} e^{-0.15z} \text{ s}^{-1} \qquad (1)$$

and the unperturbed electron density profile given by

$$N_e(z) = 7.857 \times 10^{-5} e^{\beta(z-H')} \nu(z) \text{ cm}^{-3}, \qquad (2)$$

where we take β = 0.43 km^{-1} and H' = 87 km [*Wait and Spies*, 1964]. The ambient magnetic field is assumed to have a strength of 3.8×10^{-5} T and a co-dip angle of 130°. The LIE is defined by the quantity $\delta N_e(x, y, z)$ or the perturbation of electron density. The perturbation of collision frequency $\delta\nu(x, y, z)$ due to heating is assumed zero due to the rapid cooling of the plasma within a timescale ~ms [*Rodger et al.*,

1998]. The LIE may then be defined as a spatial perturbation of susceptibility tensor $\chi'(x, y, z)$. LIE electron density profile $\delta N_e(x, y, z)$ is rather arbitrarily assumed here to be independent of horizontal coordinates x and y but confined to an ellipse with the long axis magnetic E/W. The ratio of major axis to minor axis of the ellipse is taken to be 2.5 in accordance with the previous discussion. The vertical dependence of electron density perturbation is assumed to be Gaussian, centered at a height z_o with a variance σ. In the vertical direction the LIE is limited to the height range 60–95 km. The top height of 95 km is above the reflection level, and scattering from above this height may be neglected. The electron density perturbation (δN_e) above the ambient profile is given by

$$\delta N_e = \delta N_e^0 \exp^{[(z-z_0)^2/\sigma^2]} F(x', y'), \qquad (3)$$

where δN_e^0 is the perturbation at the patch center, x' is the local E/W coordinate, and y' is the N/S coordinate. Here F is unity inside the ellipse and zero outside it. In the present simulation we take z_0 to be in the range 80–87 km and σ = 10 km. The short semiaxis is taken to be 400 km and the long semiaxis 1000 km, that is, the LIE ellipse is 2000 km long and 800 km wide. The maximum electron density perturbation δN_e^0 at the LIE center is taken to be 1.5 el cm^{-3}, consistent with precipitating electron fluxes observed on low altitude orbiting satellites [*Voss et al.*, 1998; *Molchanov et al.*, 1998]. We note here that due to the transitory nature of the precipitation the satellite is unable to determine patch size.

4.2. Scattering Theory and Implementation

[24] The linear Born theory of 3D VLF scattering from an ionospheric plasma perturbation is fully described in *Nunn* [1997]. The Born approximation involves assuming that the total incident field at a given point in the LIE is the incident zero order field ($\mathbf{E_0}$). As shown by *Nunn* [1997], a better linearization may be achieved by assuming that the perturbation of electric displacement vector is zero within the LIE rather than the perturbation of electric field is zero. This takes into account the polarization field generated within the LIE, and results in the following expression for effective source current ($\mathbf{J_{eff}}(\mathbf{r})$):

$$\mathbf{J_{eff}}(\mathbf{r}) = \sigma\mathbf{E_0} = \frac{jk^2\mathbf{X'}}{\omega\mu_0}(1 + (1-\alpha)\mathbf{X_0} + \alpha\mathbf{X})^{-1}(1 + \mathbf{X_0})\mathbf{E_0}, \quad (4)$$

where $\mathbf{X_0}$ is the zero-order susceptibility tensor, $\mathbf{X'}$ is the perturbation of susceptibility tensor due to the LIE, and $\mathbf{X}$ is the total susceptibility.

[25] The quantity α is a factor dependent on the geometry of the LIE. In the current simulations the LIE resembles a flat dielectric disc. By analogy with the isotropic problems of a dielectric slab or sphere in an applied electric field a suitable choice for α is 0.66, although the results of this simulation are scarcely affected by the choice of parameter α.

[26] The current version of the code neglects all components of conductivity tensor σ except the zz component. When the transmitter and receiver are both vertical electric dipoles, this is amply justified to an overall accuracy of order a few percent. A more advanced version of this code due to R. Yeo [*Clilverd et al.*, 1999] uses the full σ matrix and by means of NOSC LWPC propagation code also
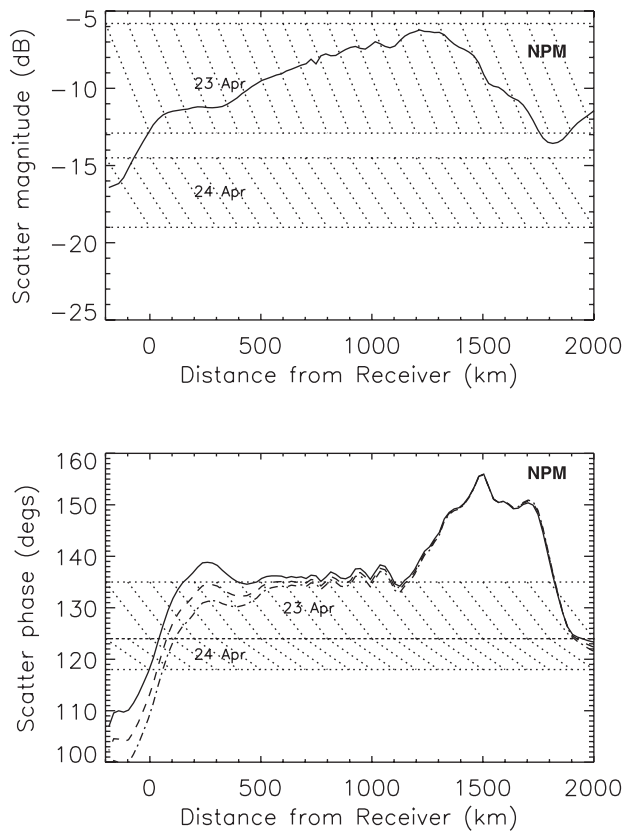
Figure 5. The variation of (top) scatter amplitude and (bottom) phase versus distance from the receiver for NPM-Faraday. The shaded areas indicate observed values on 23 and 24 April 1993.

permits an inhomogeneous background ionosphere. Clearly, for large LIE patches and/or patches with large δN_e the Born approximation will break down, since the total field at a point in the LIE will not be well approximated by the zero-order incident field. Using a 2D Finite Element modeling of VLF scattering, it was shown in *Nunn et al.* [1998] and *Baba et al.* [1998] that for an LIE with horizontal dimensions ~100 km the Born approximation fails for maximum electron density perturbations >6 electrons cm^{-3}. The dominant cause of non-Born behavior is the progressive exclusion of the incident field from the interior of the LIE due to the classic and well-known skin depth effect. When the skin depth is of the order of the vertical dimension of the LIE, then nonlinear scattering may be anticipated. The current version of the code calculates an attenuation factor for the incident field inside the LIE due to the skin depth effect, but in the present calculations, δN_e is small and the situation is fairly close to linear Born scattering.

[27] The physical volume of the LIE is enclosed by a 3D spatial box, containing a grid of $120 \times 300 \times 60$ points in x, y, z respectively. The incident field $\mathbf{E_0}$ is computed at each elemental point, from which the source current $\mathbf{J_{eff}}$ may be derived. The scattered field is that radiated by the source current field $\mathbf{J_{eff}(r)}$ located within the body of the LIE. It is clearly necessary to calculate the transmissivity between the transmitter and every point in the LIE, as well as between every point in the LIE and the receiver. Transmissivity of the direct path transmitter to receiver is also

required. To handle the subionospheric VLF propagation problem the code uses the well known modal theory of *Wait* [1970]. Numerical experimentation has shown that at ranges shorter than ~50 km the modal expansion does not provide a satisfactory description of the field $\mathbf{E(r)}$, and so in this code, calculations of scattered field from LIE elements closer than ~50 km to the receiver will be subject to some inaccuracy. However due to the rapid variation of scatter phase with element position in the immediate vicinity of the receiver scatter field strength will be low for areas of the LIE directly overhead the receiver. The code uses the NOSC MODEFNDR [*Morfitt and Shellman*, 1976] suite of programs in order to compute VLF modal propagation. These codes incorporate Earth curvature and an anisotropic ionosphere, and a ground-plane of specified conductivity and dielectric constant. These programs have the disadvantage of being inaccurate at very high altitudes >90 km, and future research involving either short ranges or scattering from high altitudes should have transmissivities calculated from a full wave VLF program. For the NPM, NAA, NSS, and NLK transmitters, MODEFNDR returns 19, 21, 20, and 23 modes respectively. These include both TM and TE modes, and all are used in the propagation calculations. Even for the scattered field, which has a short range, the highest-order modes are highly attenuated and were found to have negligible amplitudes at the receiver, thus confirming the validity of the modal expansion.

4.3. Modeling Results

[28] The results from the code are presented in Figures 5, 6, 7, and 8. The center of the E-W orientated elliptical LIE is
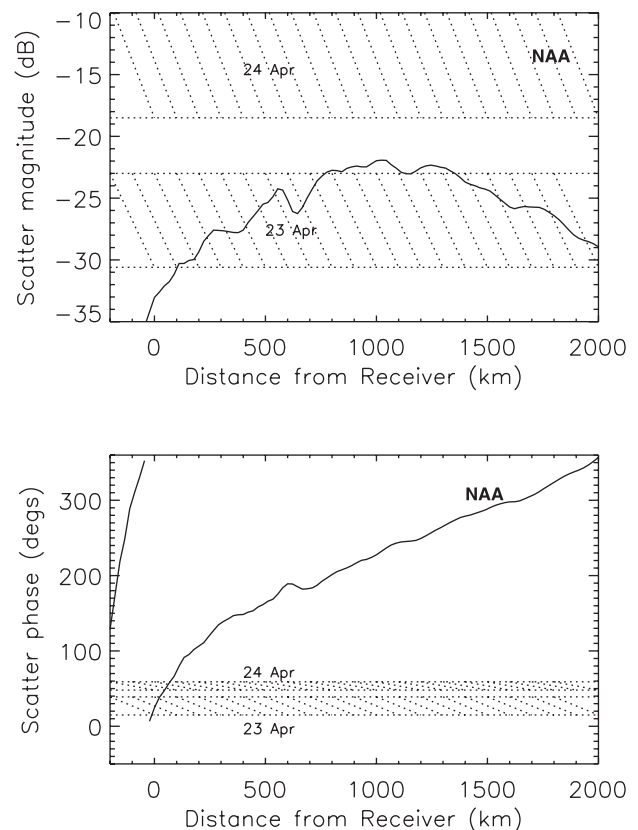

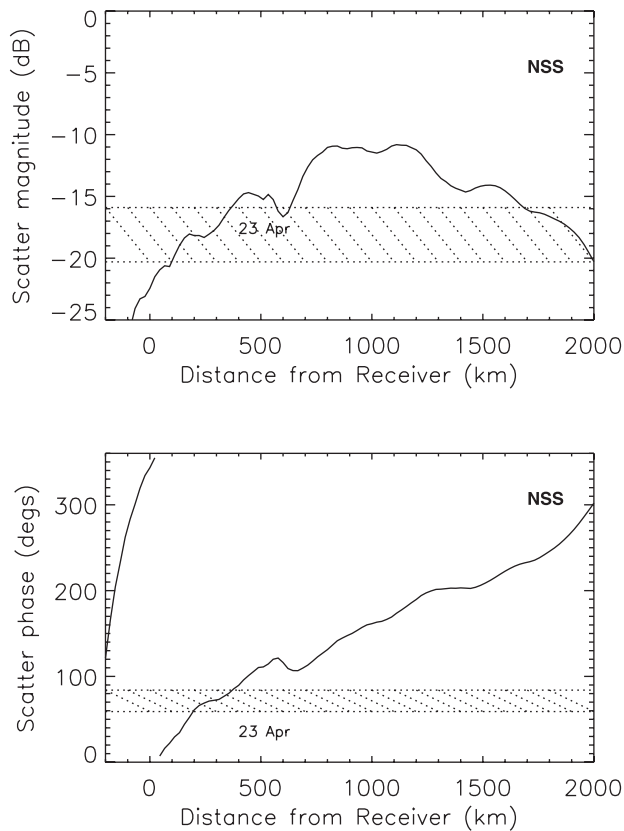**Figure 6.** As Figure 5 but for NAA-Faraday.

Figure 7.   As Figure 5 but for NSS-Faraday.

the path but being further from the receiver the resultant scatter amplitude is smaller. The scatter phase for NPM-Faraday is shown by a solid line (lower panel). An increase in phase occurs as the distance from Faraday is increased, from ~110° at 0 km to about 150° at 1500 km, although there is little variation in phase between 300 and 1000 km.

[31]   The model results can be compared with the scatter values given in Table 2 for NPM-Faraday. On 23 April 1993 the scatter amplitude values range from −5.8 to −12.9 dB and are represented on the plot by a hatched region that overlaps the line at patch center distances of 0−2000 km from the receiver. The scatter phase values range from 124° to 135°. These are equivalent to distances of ~200− 1100 km. On 24 April 1994, where there was some evidence that the patches appeared to be situated more eastward than on 23 April 1994, we see that the lower amplitudes and lower phases are consistent with the center of the patches being within 100−200 km of Faraday.

[32]   Figure 6 shows the effect of the patch location on the NAA-Faraday path. The variation of scatter amplitude and phase with distance are similar to that for NPM-Faraday. When the center of a patch is overhead of Faraday the amplitudes are about −35 dB and the phase is close to 0°. The phase values for NAA-Faraday from Table 2 indicate that on 23 and 24 April the latitudinal midpoint of the patches were close to overhead at Faraday. The scatter amplitudes on 23 April mainly have values of −30 dB, which is also consistent with patches close to the receiver. However, on 24 April the scatter magnitudes are well above the modeled results. One possiblilty is that within the
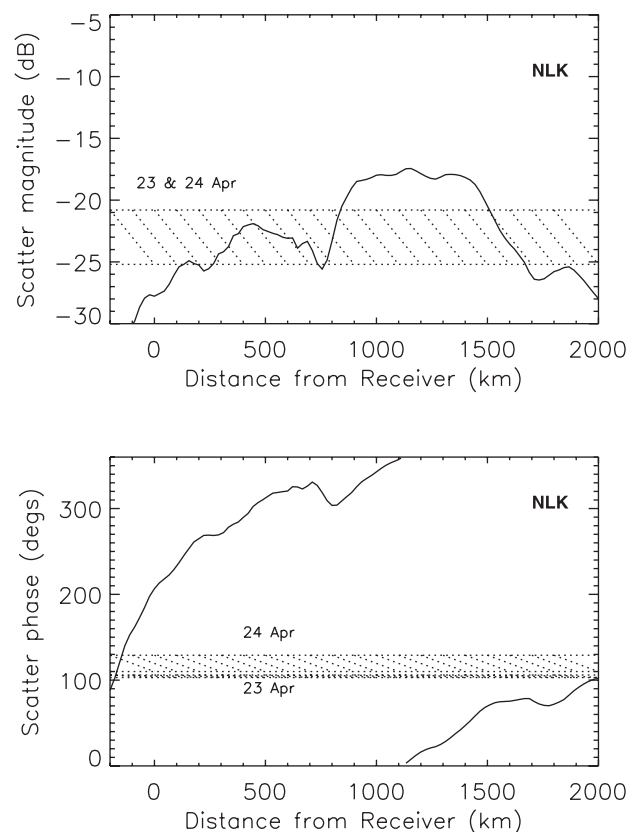
moved along the GCP from −200 km from the receiver (i.e. behind the receiver) out to a range of 2000 km, in steps of 10 km. Both scatter magnitude (decibels) and scatter phase (degrees) are plotted against distance. Figure 5 represents the calculations for NPM received at Faraday. The scatter amplitude (solid line, upper panel) increases with patch center distance from the receiver until ~1200 km when values of −6 dB occur. This result upholds our initial assumption that the Trimpi perturbation size is proportionally related to the amount of the GCP on which precipitation is occurring, at least, for the 1000 km of the path nearest to the receiver.

[29]   At greater distances than this the amplitude falls to values of −14 dB at ~1800 km, because the LIE-receiver range is increasing. The calculated Trimpi amplitudes are very closely proportional to the electron density perturbation of the LIE (δN_e^0). Thus a doubling of LIE density gives a +6 dB increase in Trimpi magnitude. Calculated Trimpi phases are almost independent of LIE density, as shown by the lower panel in which 1, 3, and 5 electrons cm^{-3} phase results are plotted to provide an idea of the variability.

[30]   The distance at which the maximum amplitude occurs is dependent on the dimensions of the patch. In this case the NPM-Faraday path is oriented east-west through the major axis of the patch. When the center is 1000 km from Faraday, the eastern edge is overhead at Faraday. If the patch is moved toward Faraday then some of the patch will be eastward of the receiver and have little influence, thus the amplitude is less for distances less than 1000 km. For distances greater than 1000 km, the whole patch influences

Figure 8.   As Figure 5 but for NLK-Faraday.

patches there are regions of increased density, in this case by a factor of ~4 (or 6 electrons cm^{-3}).

[33] The model calculations for the NSS-Faraday path are shown in Figure 7. The nearest equivalent data set in Table 2 is NSS-Rothera. As the Rothera receiver is 300 km farther poleward than Faraday, the patch center estimate will be 300 km larger on the graphs. Thus, for amplitude values of between −15 and −20 dB, and phases of 60°–80°, distances of 200–400 km from Rothera are indicated. This is equivalent to the patch being overhead close to the longitude of Faraday, as estimated using NAA-Faraday. Limited amounts of data are available for NSS-Palmer, which is a close equivalent to NSS-Faraday. Amplitudes of ~−20 dB and phases of ~310° are indicative of near overhead patches in agreement with the other estimates.

[34] From Figure 7 it is also possible to estimate the amplitude and phase of NSS-Halley Trimpi events. This assumes similar modal make-up along the NSS GCPs to Halley and Faraday. The distance from the point where the $L = 2.5$ contour crosses the NSS-Halley GCP to the Halley receiver is ~2000 km. Using this distance in Figure 7, we find that the calculated scatter amplitude is −20 dB and the phase is 300°. These values are in good agreement with those for NSS-Halley in Table 2. This result was confirmed in a separate computation in which a circular LIE was placed on the Halley-NSS GCP with a latitudinal dimension of 500 km at a range of 1850 km from Halley. The calculated Trimpi had a scatter amplitude of −20.4 dB and a scatter phase of 314°.

[35] The scatter values for NLK-Faraday are shown in Figure 8. The Trimpi data from NLK-Palmer is equivalent in this case. Amplitude values of −23 dB for 23 April and −22 dB for 24 April give a wide range of distances of the patches from the receiver (200–1600 km). However phase values of ~110° suggest that the patch midpoint is within 200 km of the receiver. The NLK-Rothera data show similar amplitudes and slightly higher phases to NLK-Palmer which is consistent with patch centers further from Rothera than Palmer/Faraday.

5. Discussion

[36] Using Trimpi events observed on many transmitter–receiver GCPs, we have estimated precipitation patches to be large, i.e., at least 1500 km × 600 km, with the longer axis oriented east-west. Calculations using a 3-D Born scattering model provides results which are consistent with this picture, where patch densities are 1.5 electrons cm^{-3} above ambient at ~84 km. There were a high proportion of the Trimpi events during 0500–1100 UT on 23 and 24 April 1994, which could be associated with strong lightning flashes (those with high peak return stroke currents) in eastern United States. Thus we are even more confident that the Trimpi observed were caused by field-aligned electron precipitation. But is it possible to determine if the Trimpi events were caused by ducted or nonducted VLF waves?

[37] The nonducted wave mechanism proposed by *Lauben et al.* [1999] and *Johnson et al.* [1999] does not require the presence of an associated conjugate-hemisphere whistler. However, the ducted wave mechanism would produce an amplified field-aligned whistler signal that will probably

penetrate the ionosphere in the conjugate hemisphere and may be observed on the ground. Broadband recordings (0.5–10 kHz) were made synoptically at Faraday for 1 min at 05, 20, 35, and 50 min past each hour of the day. Only 2 Trimpi events, of the 47 where we know the location of the >100 kA causative discharge, occurred during these minutes. Neither event could be associated with a whistler. Broad band recordings were also made at Palmer, where whistlers were also absent prior to several other Trimpi events that occurred during recording times. However, if the whistlers were penetrating through the ionosphere close to the center of the precipitation patch they would be at least 700 km from the receivers (probably 200–400 km more if, as expected, the whistlers exit equatorwards of the field line on which they propagate) and would thus be expected to be very faint, possibly undetectable [*Smith et al.*, 2001].

[38] The patch dimensions determined by the nonducted whistler mechanism are ~1200 km × ~450 km. This estimate is made from the figures of *Johnson et al.* [1999], but ignores the contribution to the patch size of ionisation occurring at higher L shells than $L = 3.0$. Above $L = 3.0$ precipitating electrons would tend to be less energetic and be unable to penetrate below the D region and would thus not influence any transmitter-receiver GCPs [*Clilverd et al.*, 1999]. The patch dimensions are similar to those determined in this paper. The distance from the causative discharge to the lowest latitude of the patch in the work of *Johnson et al.* [1999] was 7° in latitude or 700–800 km. The events studied in this paper had causative discharges at 34°N. Thus the lowest latitude of the patch would be predicted to be at the conjugate region to 41°N (near 75°W), i.e., at 67°S, 80°W. This location is significantly poleward of the position estimated for the events studied in this paper, where the lower latitude boundary is close to the conjugate latitude of the causative lightning ~60°S. However, this picture was developed for lightning and precipitation occurring in the same hemisphere and may not be truly representative of the opposite hemisphere to the causative lightning. Additionally, *Johnson et al.* [1999] found that they had to shift the location of the precipitation patch slightly equatorward of that predicted in order to reproduce their Trimpi data in the Northern Hemisphere. Further modeling studies of the kind described by *Lauben et al.* [1999] would help clarify this point. Another characteristic of the nonducted whistler mechanism would be to see systematically changing onset delay times for different paths studied. The time resolution used in this study is too large to provide any information about the relative time delays.

[39] Fully ducted VLF waves would produce electron precipitation patches of the size of the duct in the wave interaction region near the equatorial plane. Evidence for small (~100 km) duct sizes is compelling [*Strangeways*, 1999]. Thus it is unlikely that the patch dimensions determined in this study are due to fully ducted waves. However, *Strangeways* [1999] suggests a mechanism in which field-aligned VLF waves near the equatorial plane radiate power into modes with larger wave normal angles to the geomagnetic field direction. This results in larger regions from which precipitating electrons arise, particularly poleward of the duct center. This mechanism also predicts elliptical patch shapes, rather than circular. As some of the wave energy would remain ducted a whistler occurring in the

conjugate hemisphere would be possible. The lack of whistlers recorded at Faraday and Palmer in this study would argue against this mechanism. Further, it is unclear why, when lightning signals can propagate up to ~1000 km before entering a duct [*Carpenter and Orville*, 1989], the lightning in this study appears to cluster close to the center of the precipitation region. On the other hand, whistlers trapped into ducts are likely to be generated by lightning which is $1-1.5°$ equatorward of the duct center [*Strangeways*, 1981]. This would produce a patch of precipitation with a lower latitude boundary close to the conjugate latitude of the lightning, which is consistent with the findings of this paper. We should also note that ducted whistlers have been observed in association with Trimpi events many times in the past.

[40] Early work on Trimpi events observed from Faraday and Halley was undertaken by *Smith et al.* [1993], using lower (10–14 kHz) frequency OMEGA transmissions. Small precipitation patch dimensions were inferred on a similar set of paths to those studied in this paper. Primarily, this was because >95% of the events were noncoincident, and hence the patches had to be small so that they did not interact with the other paths. However, the inferred locations of the precipitation on each path is almost identical to those inferred in this paper. One can only assume that the higher lightning noise levels at the frequencies studied made the observation of coincident Trimpi events much more difficult than with the present equipment and frequencies used.

[41] *Smith et al.* [2001] used whistler occurrence rates to estimate the effectiveness of whistler-induced electron precipitation compared with radiation belt losses due to hiss. This work followed on from previous estimates made by *Burgess and Inan* [1993]. Hiss was estimated to be about a factor of 10 more effective than ducted whistlers in depleting the radiation belts. However, the precipitation area used was ~1800 times smaller than that estimated in this paper. Using the larger area would make lightning ~10–100 times more effective than hiss in depleting the radiation belts.

6. Summary

[42] Using Trimpi events observed on many transmitter-receiver GCPs, we have estimated precipitation patches to be large, i.e., ~1500 km × 600 km, with the longer axis oriented east-west. Calculations using a 3-D Born scattering model provides results which are consistent with this picture, where patch densities are 1.5 electrons cm^{-3} above ambient at ~84 km. The model results confirmed the assumption made that the size of the perturbation on the transmitter-receiver GCP was proportional to the length of the path influenced by precipitation, at least when the precipitation was close to the receiver end of the path.

[43] A high proportion (38%) of the Trimpi events were associated with strong lightning flashes in eastern United States. The remainder of the events were likely to have been caused by lightning farther eastward and out to sea thus being undetected by the NLDN data set used in this study. When lightning discharges had currents >65 kA (positive or negative), there was a >80% chance of seeing an associated Trimpi event. The chance of seeing any Trimpi events falls to zero for discharges of <45 kA.

[44] The strongest Trimpi perturbations occur when the center of the precipitation patch is ~1000 km from the receivers, which represents the case when the edge of the precipitation patch is overhead at the receiver. This was shown when the latitude and longitude of lightning discharges produced the most significant (S/N) Trimpi events on NPM-Faraday when they occurred at 34°N, 76°W. The magnetic conjugate to this location is 60°S, 80°W, which is ~700 km from Faraday. This result is consistent with the modeling calculations for large patches.

[45] The equatorward edge of the precipitation patch was estimated to be at about 60°S, close to the magnetic conjugate of the lightning. Nonducted whistler precipitation mechanisms would predict a $5°-10°$ latitudinal gap between the lightning and the equatorward edge of the patch [*Johnson et al.*, 1999]. However, this picture was developed for both lightning and precipitation occurring in the same hemisphere and may not be truly representative of precipitation in the opposite hemisphere to the causative lightning. The size of the patch estimated in this study is consistent with the size of patches predicted by nonducted whistler precipitation. The lack of observed whistlers at the time of the Trimpi events, on the few occasions where recordings were being made, is also consistent with the nonducted whistler mechanism.

[46] The close association of the equatorwards edge of the precipitation patch with the conjugate location of the causative lightning is consistent with the quasi-ducted mechanism suggested by *Strangeways* [1999]. The size and elliptical nature of the precipitation patch predicted is also consistent with the dimensions determined in this study. The lack of observation of whistlers in the opposite hemisphere to the lightning is however, not consistent with the proposed mechanism, although the distances from duct exit point to receiver may have been too large (~700 km) for the signals to propagate detectably.

[47] The precipitation of electrons (~100 keV) from the radiation belts is dependent on the size of the precipitation patch, which is a result of mapping from the cross-sectional area of the wave-particle interaction region to the ionosphere. Using the significantly larger patch dimensions determined in this study, it is estimated that lightning may well be 10–100 times more effective at depleting the radiation belts than hiss.

References

Baba, K., D. Nunn, and M. Hayakawa, The modelling of VLF Trimpis using both finite element and 3D Born modelling, *Geophys. Res. Lett.*, *25*, 4453–4456, 1998.

Burgess, W. C., and U. S. Inan, Simultaneous disturbance of conjugate ionospheric region in association with individual lightning flashes, *Geophys. Res. Lett.*, *17*, 259–262, 1990.

Burgess, W. C., and U. S. Inan, The role of ducted whistlers in the precipitation loss and equilibrium flux of radiation belt electrons, *J. Geophys. Res.*, *98*, 15,643–15,665, 1993.

Carpenter, D. L., and R. E. Orville, The excitation of active whistler mode signal paths in the magnetosphere by lighting, 2, Case studies, *J. Geophys. Res.*, *94*, 8886–8894, 1989.

Clilverd, M. A., R. F. Yeo, D. Nunn, and A. J. Smith, Latitudinally dependent Trimpi effects: modelling and observations, *J. Geophys. Res.*, *104*, 19,881–19,887, 1999.

Crombie, D. D., The effects of a small local change in phase velocity on the propagation of a VLF radio signal, *J. Res. Natl. Bur. Stand. U.S., Sect. D*, *68*, 1964.

Cummins, K. L., M. J. Murphy, E. A. Bardo, W. L. Hiscox, R. B. Pyle, and A. E. Pifer, A combined TOA/MDF technology upgrade of the US national lightning detections network, *J. Geophys. Res.*, *103*, 9035–9044, 1998.

Dowden, R. L., and C. D. D. Adams, Phase and amplitude perturbations on subionospheric signals explained in terms of echoes from lightning-induced electron precipitation ionization patches, *J. Geophys. Res.*, *93*, 11,543–11,551, 1988.

Dowden, R. L., and C. D. D. Adams, Phase and amplitude perturbations on the NWC signal at Dunedin from Lightning induced electron precipitation, *J. Geophys. Res.*, *94*, 497–503, 1989.

Dowden, R. L., and C. D. D. Adams, Size and location of lightning-induced enhancements from measurement of VLF phase and amplitude perturbations on multiple antennas, *J. Atmos. Terr. Phys.*, *55*, 1335–1359, 1993.

Dowden, R. L., C. D. D. Adams, J. B. Brundell, and P. E. Dowden, Rapid onset, rapid decay (RORD), phase and amplitude perturbations of VLF subionospheric transmissions, *J. Atmos. Terr. Phys.*, *56*, 1513–1527, 1994.

Dowden, R. L., C. J. Rodger, J. Brundell, and M. A. Clilverd, Decay of whistler-induced electron precipitation and cloud-ionosphere electrical discharge Trimpis: Observations and analysis, *Radio Sci.*, *36*, 151–169, 2001.

Helliwell, R. A., J. P. Katsufrakis, and M. L. Trimpi, Whistler-Induced amplitude perturbations in VLF propagation, *J. Geophys. Res.*, *78*, 4679–4688, 1973.

Inan, U. S., T. G. Wolf, and D. L. Carpenter, Geographic distribution of lightning-induced electron precipitation observed as VLF/LF perturbation events, *J. Geophys. Res.*, *93*, 9841–9854, 1988.

Ingmann, P., J. Schaefer, H. Volland, M. Schmolder, and A. Manes, Remote-sensing of thunderstorm activity by means of VLF sferics, *Pure Appl. Geophys.*, *123*, 155–170, 1985.

Johnson, M. P., U. S. Inan, and D. S. Lauben, Subionospheric VLF signatures of oblique (nonducted) whistler-induced precipitation, *Geophys. Res. Lett.*, *26*, 3569–3572, 1999.

Lauben, D. S., U. S. Inan, and T. F. Bell, Poleward-displaced electron precipitation from lightning-generated oblique whistlers, *Geophys. Res. Lett.*, *26*, 2633–2636, 1999.

Lev-Tov, S. J., U. S. Inan, and T. F. Bell, Altitude profiles of localised D-region density disturbances produced in lightning-induced electron-precipitation events, *J. Geophys. Res.*, *100*, 21,375–21,383, 1995.

Lev-Tov, S. J., U. S. Inan, A. J. Smith, and M. A. Clilverd, Characteristics of localized ionospheric disturbances inferred from VLF measurements at two closely spaced receivers, *J. Geophys. Res.*, *101*, 15,737–15,747, 1996.

Molchanov, O. A., A. V. Shvets, and M. Hayakawa, Analysis of lightning-induced ionization from VLF Trimpi events, *J. Geophys. Res.*, *103*, 23,443–23,453, 1998.

Morfitt, D. G., and C. H. Shellman, MODESRCH, an improved computer program for obtaining ELF/VLF mode constants, *Tech. Rep. NOSC/TR 141*, NTIS, ADA 032473, Nav. Electron. Lab. Cent., San Diego, Calif., 1976. (Available as *ADA047508* from Natl. Tech. Inf. Serv., Springfield, Va.)

Nunn, D., On the numerical modelling of the VLF Trimpi effect, *J. Atmos. Sol. Terr. Phys.*, *59*, 537–560, 1997.

Nunn, D., K. Baba, and M. Hayakawa, VLF Trimpi modelling on the path NWC-Dunedin using both finite element and 3D Born modelling, *J. Atmos. Sol. Terr. Phys.*, *60*, 1497–1515, 1998.

Nunn, D., and C. J. Rodger, Modelling the relaxation of red sprite plasma, *Geophys. Res. Lett.*, *26*, 3293–3296, 1999.

Nunn, D., and H. J. Strangeways, Trimpi perturbations from large ionisation enhancement patches, *J. Atmos. Sol-Terr. Phys.*, *62*, 189–206, 2000.

Poulsen, W. L., T. F. Bell, and U. S. Inan, The scattering of VLF waves by localised ionospheric disturbances produced by lightning induced electron precipitation, *J. Geophys. Res.*, *98*, 15,553–15,559, 1993.

Rodger, C. J., O. A. Molchanov, and N. R. Thomson, Relaxation of transient ionization in the lower ionosphere, *J. Geophys. Res.*, *103*, 6969–6975, 1998.

Rodger, C. J., Red sprites, upward lightning, and VLF perturbations, *Rev. Geophys.*, *37*, 317–335, 1999.

Rodger, C. J., and D. Nunn, VLF scattering from red sprites: Application of numerical modelling, *Radio Sci.*, *34*, 933–938, 1999.

Smith, A. J., P. D. Cotton, and J. S. Robertson, Transient 10 s VLF amplitude and perturbations due to lightning-induced electron precipitation into the ionosphere 'the Trimpi effect', *AGARD Conf. Proc.*, *529*, 1993.

Smith, A. J., Aspects of wave-particle interactions at mid-latitudes, *Adv. Space Res.*, *17*, 213–222, 1996.

Smith, A. J., M. B. Grieve, M. A. Clilverd, and C. J. Rodger, A quantitive estimate of the ducted whistler power within the outer plasmasphere, *J. Atmos. Sol. Terr. Phys.*, *63*, 61–74, 2001.

Strangeways, H. J., Determination by ray-tracing of the regions where mid-latitude whistlers exit from the lower ionosphere, *J. Atmos. Terr. Phys.*, *43*, 231–238, 1981.

Strangeways, H. J., Lightning induced enhancements of D region ionisation and whistler ducts, *J. Atmos. Sol. Terr. Phys.*, *61*, 1067–1080, 1999.

Tolstoy, A., and T. J. Rosenberg, Model predictions of subionospheric VLF signal perturbations resulting from localised electron precipitation induced D region ionisation enhancement regions, *J. Geophys. Res.*, *91*, 13,473–13,482, 1986.

Voss, H. D., M. Walt, W. L. Imhof, J. Mobilia, and U. S. Inan, Satellite observations of lightning-induced electron precipitation, *J. Geophys. Res.*, *103*, 11,725–11,744, 1998.

Wait, J. R., *Electromagnetic Waves in Stratified Media*, Pergamon, New York, 1970.

Wait, J. R., and K. P. Spies, Characteristics of the Earth-ionosphere wave-guide for VLF radio waves, *NBS Tech. Note 300*, 1964.

Wolf, T. G., and U. S. Inan, Path-dependent properties of subionospheric VLF amplitude and phase perturbations associated with lightning, *J. Geophys. Res.*, *95*, 20,997–21,005, 1990.

————————

M. A. Clilverd and A. J. Smith, Physical Sciences Division, British Antarctic Survey, Madingley Road, Cambridge, CB3 0ET, England, UK. (m.clilverd@bas.ac.uk; a.j.smith@bas.ac.uk)

R. L. Dowden, LF.EM Research, 17 Dunedin-Waitai Hwy, Pine Hill, Dunedin, New Zealand. (dowden@physicist.net)

U. S. Inan and S. J. Lev-Tov, STAR Lab, 306 Packard Building, Stanford, CA 94303, USA. (inan@nova.stanford.edu; sjlt@stanford.edu)

D. Nunn, Department of Electronic and Computer Science, University of Southampton, Southampton, SO17 1BJ, England, UK. (dn@ecs.soton.ac.uk)

C. J. Rodger, Department of Physics, University of Otago, Dunedin, New Zealand. (crodger@physics.otago.ac.nz)